Compressive spectral imaging via misalignment induced equivalent grayscale coded aperture

Tong Zhang, Shengjie Zhao, Senior Member, IEEE, Xu Ma, Senior Member, IEEE, Andres Ramirez-Jaime, Qile Zhao, and Gonzalo R. Arce, Fellow, IEEE

Abstract—Coded aperture snapshot spectral imager (CASSI) senses the spectral information of a 2D scene and captures a set of coded measurement data that can be used to reconstruct the 3D spatio-spectral datacube of the input scene by compressive sensing algorithms. The coded aperture (CA) in CASSI plays a crucial role in modulating the spatial information. The pixels in CA are typically square, switched binary on-off, and aligned with the pixels of focal plane array (FPA). Instead of this binary modulation, this paper explores a simple yet effective approach to enabling an equivalent grayscale modulation, which can increase the sensing degree of freedom in CASSI systems. In particular, we deliberately introduce misalignment between the CA pixels and the FPA pixels, such that the spatial modulation of one FPA pixel is determined by four adjacent CA pixels instead of one. Numerical experiments show that the proposed equivalent grayscale modulation induced by misalignment can significantly improve the CASSI reconstruction when compared with current methods, whether a random CA or an optimal blue noise CA is used. More importantly, it does not incur in any cost to the CASSI system.

Index Terms—Computational imaging, multispectral and hyperspectral imaging, coded aperture imaging.

I. Introduction

Spectral imaging captures the spectral information across multiple wavelength bands and provides a 3D spatio-spectral datacube of the input scene [1], [2]. Traditional spectral imaging approaches construct the datacube by scanning the scene along either the spatial or the spectral dimensions. Growing demand for finer spatio-spectral resolution poses challenges to this approach on acquisition time, data volume size, and imaging system complexity [3]. An emerging alternative is compressive spectral imaging (CSI), which exploits the redundancy of the spatio-spectral datacube and captures both the spatial and spectral information of the input scene based on the theory of compressive sensing [4]. The coded aperture snapshot spectral imager (CASSI) proposed by Wagadarikar et al. is a typical CSI system [5]. As shown in Fig. 1, the input scene is spatially encoded by the block/unblock coded aperture (CA) and spectrally shifted by the prism, and then captured by the 2D focal plane array (FPA), which mixed together the coded spatial and spectral information of the scene. The imaging lens in CASSI system is used to form an intermediate real image for modulation while the relay lenses are used to project the encoded scene to the 2D FPA. Subsequently, reconstruction algorithms for compressive sensing problem are used to recover the underlying 3D spatio-spectral datacube of the input scene. Assuming that the spectral scene is resolved into $M \times N$ spatial pixels and L wavelength bands, then the measurement data captured by the FPA in a single snapshot has a size of $M \times (N - L + 1)$, which in some cases is not enough to recover the 3D spatio-spectral datacube. To overcome this problem, CASSI system usually takes multiple snapshots with different CA patterns to obtain sufficient measurement data [6]. Generally, the multiple modulations are realized by using a digital micromirror device (DMD) in CASSI system, where the micromirrors are programmable and can quickly switch their block/unblock setting at each snapshot [6].

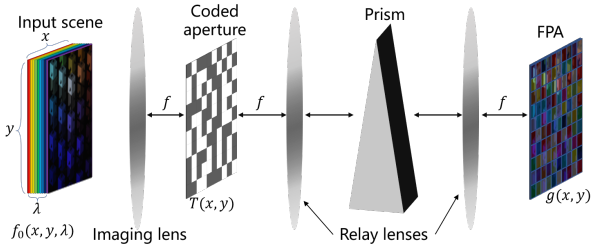

Fig. 1: Structure of CASSI system.

The modulation elements such as the CA and disperser device play a crucial role in the CASSI system, as they determine the capability to sense the spatio-spectral information, which in turn affects the reconstruction performance. Arguello et al. developed a higher-order

T. Zhang, and S. Zhao were supported in part by the National Key Research and Development Project under Grant 2019YFB2102300, in part by the National Natural Science Foundation of China under Grant 61936014, in part by Fundamental Research Funds for the Central Universities, in part by Shanghai Municipal Science and Technology Major Project No. 2021SHZDZX0100. (Corresponding author: Shengjie Zhao). G. R. Arce was supported by the National Science Foundation (NSF) (CIF 1717578).

T. Zhang is with the School of Software Engineering, Tongji University, Shanghai, 201804, China (email: tongzhang@tongji.edu.cn).

S. Zhao is with the School of Software Engineering, Tongji University, China, and also with the Key Laboratory of Embedded System and Service Computing, Ministry of Education, Tongji University, Shanghai, 201804, China (email: shengjiezhao@tongji.edu.cn).

A. Ramirez-Jaime and G. R. Arce are with the Department of Electrical and Computer Engineering, University of Delaware, Newark, DE 19716 USA (email: aramjai@udel.edu; arce@udel.edu).

X. Ma and Q. Zhao are with the Key Laboratory of Photoelectronic Imaging Technology and System of Ministry of Education of China, School of Optics and Photonics, Beijing Institute of Technology, Beijing 100081, China (e-mail: maxu@bit.edu.cn; qile.zhao@outlook.com).

discretization model for CASSI that takes into account the intervoxel interference caused by the prism effect and thus leads to the image reconstructions less dependent on system calibration [7]. Fu et al. optimized the sensing process of CASSI system by introducing a polar CA design [8], which can produce multiple measurements by rotation. Kar et al. proposed a novel design for CASSI system by using a diffractive lens for both dispersion and focusing [9]. The measurement diversity using multiple snapshots can be achieved by changing the focusing behavior of the diffractive lens. Recently, Zhang et al. proposed to use a CA with hexagonal pixels instead of traditional square pixels in CASSI system [10]. The mismatch between the hexagonal CA pixels and the square FPA pixels introduces equivalent grayscale modulation, which improves the system's sensing freedom. However, the hexagonal CA is currently customized and not effectively compatible with the widely used high-speed light modulation devices such as DMD and spatial light modulator (SLM).

To overcome this limitation, this letter proposes a simple yet effective approach to improving the sensing freedom of CASSI system. Instead of using any advanced device, we achieve the equivalent grayscale modulation by introducing a misalignment between the CA and the FPA. As a result, each voxel in the spatio-spectral datacube is spatially encoded by four adjacent pixels rather than one single pixel on the CA, which increases the sensing freedom of the CASSI system. Two methods for introducing this misalignment are proposed and modeled in this letter, including the subpixel translation of CA and the rotation of CA. Extensive numerical experiments are conducted to illustrate the benefit of the proposed methods. Considering that the optimal CA for multiple snapshots CSI coincides with the spatiotemporal blue noise CA under the framework of compressive sensing theory [6], [10], we also evaluate the proposed method on CA with a blue noise pattern and find that it is able to improve the performance of CASSI system without adding any hardware cost.

The rest of this letter is organized as follows. Section 2 describes the detail of the proposed methods. Section 3 presents the numerical experiments to assess the proposed method. Section 4 provides the conclusions.

II. Method

A. Forward model and inverse model of CASSI system

Denote the spatio-spectral intensity of the input scene as $f(x, y, \lambda)$, where (x, y) are the spatial coordinates and λ is the spectral coordinate. As shown in Fig. 1, $f(x, y, \lambda)$ is firstly spatially encoded by the CA, then dispersed by the prism, and finally captured by the FPA, which integrates the incident photons over the spectral sensitivity range of the detector. The resulting measurement of the CASSI system can be formulated by

$$g(x,y) = \iiint T(x',y') f(x',y',\lambda) \\ h(x'-\alpha\lambda-x, y'-y)dx'dy'd\lambda, \tag{1}$$

where $T(x', y')$ denotes the CA's transmittance, $h(x' - \alpha\lambda - x, y' - y)$ denotes the system's optical impulse response, and $\alpha\lambda$ denotes the shift introduced by the prism assuming a linear dispersion [6].

Considering that measured data by the FPA is spatially discretized, we rewrite (1) into the following discretized form

$$\mathbf{G}^k_{m,n} = \sum_{l=1}^{L} \mathbf{F}_{m,n+l,l} \mathbf{T}^k_{m,n+l} + \mathcal{E}^k_{m,n}, \tag{2}$$

where $\mathbf{F} \in \mathbb{R}^{M\times N\times L}$ is a 3D spatio-spectral datacube with the voxel $\mathbf{F}_{m,n,l}$ denoting the optical intensity of discretized input scene at the spatial coordinates (m, n) and the lth spectral band. $\mathbf{T} \in \mathbb{R}^{M\times N}$ denotes the CA with the element $\mathbf{T}_{m,n}$ being the transmittance of pixel (m, n) in CA, $\mathbf{G} \in \mathbb{R}^{M\times(N+L-1)}$ is the measurement data with the element $\mathbf{G}_{m,n}$ denoting the measured intensity by the pixel (m, n) in FPA, $\mathcal{E}$ denotes the additive noise, and the superscript $k = 1, \cdots, K$ indicates the kth snapshot.

By rearranging the elements of $\mathbf{F}, \mathbf{T}, \mathbf{G}$ and $\mathcal{E}$, (2) can be further reformulated into a vectorial form as $\mathbf{g}^k = \mathbf{H}^k\mathbf{f} + \mathbf{e}^k$, where $\mathbf{g}^k$, $\mathbf{f}$ and $\mathbf{e}^k$ are the vectorized representations of $\mathbf{G}^k$, $\mathbf{F}$ and $\mathcal{E}^k$ respectively, $\mathbf{H}^k \in \mathbb{R}^{M(N+L-1)\times MNL}$ is a sparse matrix that simultaneously considers the effect of CA and prism in CASSI system. Taking a total of K snapshots into account, the forward model of CASSI system can be formulated as

$$\mathbf{g} = \mathbf{H}\mathbf{f} + \mathbf{e}, \tag{3}$$

where $\mathbf{g}, \mathbf{e}$, and $\mathbf{H}$ are given by the following concatenation

$$\mathbf{g} = \left[\mathbf{g}^1; \cdots; \mathbf{g}^K\right], \mathbf{e} = \left[\mathbf{e}^1; \cdots; \mathbf{e}^K\right], \mathbf{H} = \left[\mathbf{H}^1; \cdots; \mathbf{H}^K\right].$$

Assuming that the vectorized spatio-spectral datacube has a sparse representation on some basis, i.e., $\mathbf{f} = \mathbf{\Psi}\mathbf{x}$, where $\mathbf{\Psi}$ is the basis, and $\mathbf{x}$ is the resulting coefficients with few nonzero elements, then (3) can be rewritten as

$$\mathbf{g} = \mathbf{A}\mathbf{x}, \qquad \|\mathbf{x}\|_0 \ll MNL, \tag{4}$$

where $\mathbf{A} = \mathbf{H}\mathbf{\Psi}$ is the sensing matrix, and $\|\cdot\|_0$ is the ℓ_0 norm. Subsequently, the inverse model for the CASSI system can be formulated as the following optimization problem [6]

$$\mathbf{x}^* = \underset{\mathbf{x}}{\operatorname{argmin}} \frac{1}{2}\|\mathbf{g} - \mathbf{A}\mathbf{x}\|_2^2 + \tau\|\mathbf{x}\|_1, \tag{5}$$

where $\|\cdot\|_2$ and $\|\cdot\|_1$ denote the ℓ_2 norm and the ℓ_1 norm respectively, τ is a constant used for the tradeoff between the data fidelity term and regularization term. The optimal solution $\mathbf{x}^*$ for the problem (5) can be obtained using the reconstruction algorithms for compressive sensing such as GPSR and TwIST [11]. Once it is solved, the datacube can be recovered by $\mathbf{\Psi}\mathbf{x}^*$.

B. Proposed misalignment induced grayscale modulation

The grayscale modulation was shown to increase the degrees of freedom in modulation and sensing, which in turn improves the performance of image reconstruction [10]. As depicted in Fig. 2, the proposed method still uses

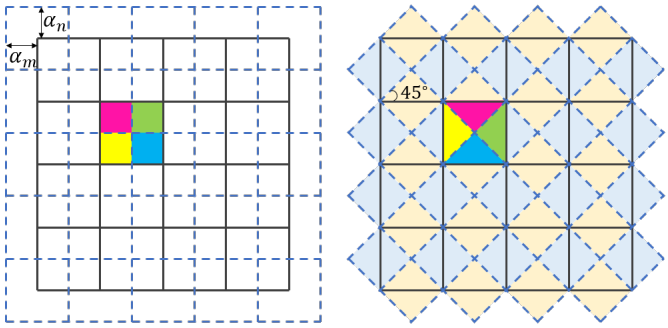

Fig. 2: Grayscale modulation introduced by misalignment between the CA and the FPA. The blue dashed lines and black solid lines represent CA and PFA, respectively. Colored patches indicate that the measurement data captured by a single FPA pixel is spatially encoded by four adjacent CA pixels rather than the single corresponding pixel in the aligned CA. (a) The grayscale modulation introduced by subpixel translation. (b) The grayscale modulation introduced by 45° rotation.

a generic CA with square pixels but exploits a deliberate misalignment between the CA and the FPA to introduce the grayscale modulation. As a result, the measured data by each FPA pixel actually is spatially encoded by four adjacent CA pixels, which exceeds the binary modulation caused by the aligned CA and FPA in a typical CASSI setup. The proposed method is more cost-effective because it is compatible with regular light modulation devices such as DMD and SLM but without requiring specialized customization. Two types of misalignment are proposed for grayscale modulation. We present the details as follows.

1) Misalignment induced by subpixel translation of CA: Misalignment can be introduced by subpixel translation between the CA and the FPA in CASSI system, which is depicted in Fig. 2(a). As a result, one FPA pixel corresponds to four adjacent CA pixels, i.e., the measured data with this FPA pixel is spatially modulated by these four CA pixels. For simplicity, we denote the regular CA with square pixels as $\mathrm{CA}_{\square}$, and the equivalent grayscale coded aperture of this type misalignment as $\mathrm{CA}_{\boxplus}$. Assuming that both CA pixels and FPA pixels have unit length, and the translation lengths of CA relative to FPA on spatial coordinates are (α_m, α_n), then the transmittance of $\mathrm{CA}_{\boxplus}$ can be calculated as

$$\begin{aligned}\mathbf{T}_{\boxplus}(m,n) = &(1-\alpha_m)(1-\alpha_n)\mathbf{T}_{\square}(m,n)\\ &+\alpha_m(1-\alpha_n)\mathbf{T}_{\square}(m+1,n)\\ &+(1-\alpha_m)\alpha_n\mathbf{T}_{\square}(m,n+1)\\ &+\alpha_m\alpha_n\mathbf{T}_{\square}(m+1,n+1),\end{aligned} \tag{6}$$

where $\mathbf{T}_{\square}$ denotes the transmittance of $\mathrm{CA}_{\square}$, and (m,n) are the spatial coordinates. That is to say, $\mathbf{T}_{\boxplus}(m,n)$ is the weighted average of the transmittance of the adjacent pixels. Although $\mathrm{CA}_{\square}$ is generally binary block/unlock switch, i.e., the elements of $\mathbf{T}_{\square}$ are either 0 or 1, the resulting pixel value of $\mathbf{T}_{\boxplus}$ actually can be 0, 1/4, 1/2, 3/4 or 1 when $\alpha_m = \alpha_n = 1/2$, which increases the freedom of sensing matrix of CASSI system.

2) Misalignment induced by 45° rotation of CA: The rotation of CA around the optical axis also can lead to misalignment and subsequently introduce the equivalent grayscale modulation. As shown in Fig. 2(b), to formulate the correspondence between the rotated CA and the FPA, we assume that the pixel spacing on CA is $1/\sqrt{2}$ of that on FPA, and the rotation angle is 45 degrees. Other settings about the rotation angle and the pixel spacing are allowed but they would increase the complexity of modeling the equivalent modulation. The rotated CA can be regarded as consisting of pixels at the odd columns (light blue squares in Fig. 2(b)) and the pixels in even columns (light yellow squares in Fig. 2(b)), and they are denoted as $\mathrm{CA}_{\square}^{\mathrm{odd}}$ and $\mathrm{CA}_{\square}^{\mathrm{even}}$, respectively. We also denote the corresponding equivalent grayscale coded aperture as $\mathrm{CA}_{\boxtimes}$. Then, the transmittance of $\mathrm{CA}_{\boxtimes}$ can be calculated as

$$\begin{aligned}\mathbf{T}_{\boxtimes}(m,n) = &\frac{1}{4}\mathbf{T}_{\square}^{\mathrm{odd}}(m,n) + \frac{1}{4}\mathbf{T}_{\square}^{\mathrm{odd}}(m+1,n)\\ &+\frac{1}{4}\mathbf{T}_{\square}^{\mathrm{even}}(m,n) + \frac{1}{4}\mathbf{T}_{\square}^{\mathrm{even}}(m,n+1),\end{aligned} \tag{7}$$

where $\mathbf{T}_{\square}^{\mathrm{odd}}$ and $\mathbf{T}_{\square}^{\mathrm{even}}$ denote the transmittance of $\mathrm{CA}^{\mathrm{odd}}$ and $\mathrm{CA}^{\mathrm{even}}$ respectively, and (m,n) are the spatial coordinates. Similar to $\mathbf{T}_{\boxplus}(m,n)$, $\mathbf{T}_{\boxtimes}(m,n)$ is also computed by the weighted average of the transmittance of the adjacent pixels, its value can be 0, 1/4, 1/2, 3/4 or 1, instead of just 0 or 1.

By using a whiteboard as the input scene and setting the CA as the chessboard pattern, we can exactly estimate the pixel shifting length (α_m, α_n) and the rotation angle by observing the constrast of the projection image.

III. Numerical experiments

In this section, we evaluate the reconstruction performance of CASSI system using the proposed misaligned coded aperture $\mathrm{CA}_{\boxplus}$ and $\mathrm{CA}_{\boxtimes}$. The regular CA with square pixels (denoted by $\mathrm{CA}_{\square}$) and the CA with hexagonal pixels (denoted by $\mathrm{CA}_{\bigcirc}$) are used for comparison. The datacube $\mathbf{F}$ consists of 256×256 pixels in spatial dimension and 24 spectral bands in the range from 450nm to 650nm. The equivalent grayscale CAs of $\mathrm{CA}_{\boxplus}$ and $\mathrm{CA}_{\boxtimes}$ have the same spatial resolution as the datacube. We use the same experiment setup as [10]. The measurement data are constructed according to (2) and taken from 10 snapshots. The CA pattern of each snapshot is randomly generated and the transmittance is set to 10%. From the multiple measurement data, we reconstruct the spatio-spectral datacube by solving (5) with the GPSR algorithm [11]. The constant τ in (5) is empirically set to 1.2e-4, 7.5e-5, 3.0e-5, and 3.0e-5 for $\mathrm{CA}_{\square}$, $\mathrm{CA}_{\bigcirc}$, $\mathrm{CA}_{\boxplus}$, and $\mathrm{CA}_{\boxtimes}$, respectively. Each spectral image in the reconstructed datacube is quantitatively evaluated using two metrics including the peak signal-to-noise ratio (PSNR) and the structure similarity (SSIM) [6].

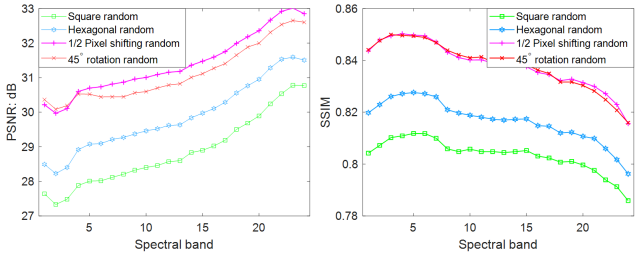

Fig. 3: Quantitative comparison of the reconstructed spectral images using different coded apertures at 24 wavelength bands. Left and right are the PSNR values and the SSIM values of the reconstructed images, respectively.

Figure 3 presents the PSNR values and SSIM values of the reconstructed spectral images that use the coded aperture $CA_{\square}$, $CA_{\bigcirc}$, $\mathbf{CA}_{\boxplus}$, and $CA_{\boxtimes}$, respectively. The corresponding average of the PSNR values at the 24 wavelength bands are 28.85dB, 29.86dB, 31.39dB, and 31.26dB, respectively. The corresponding average SSIM values are 0.8034, 0.8167, 0.8382, and 0.8381, respectively. It is found that the proposed misaligned coded apertures $CA_{\boxplus}$ and $CA_{\boxtimes}$ significantly improve the quality of reconstructed images compared to that using regular CAs with square pixels. Moreover, it also outperforms the reconstructed spectral images using the hexagonal coded aperture $CA_{\bigcirc}$, meanwhile it is easier to implement. Figure 4 presents

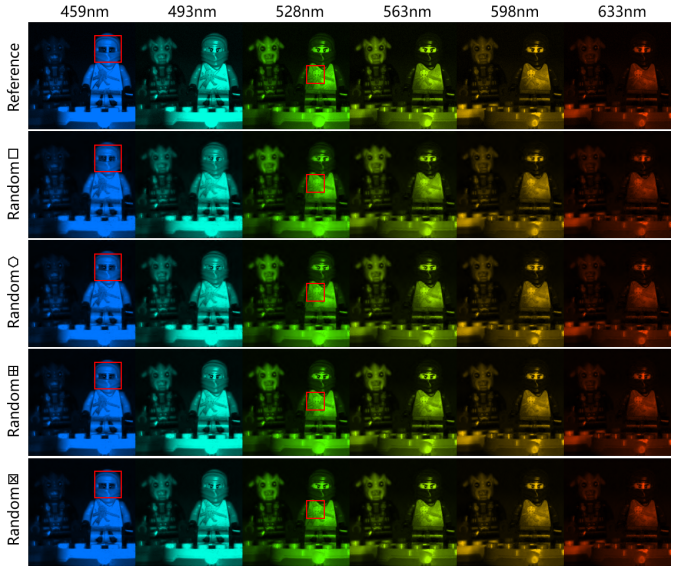

Fig. 4: Visual comparison of the reconstructed spectral images at 6 out 24 wavelength bands. Left to right: The selected wavelength bands. Top to bottom: The reference images, and the images reconstructed using random $CA_{\square}$, $CA_{\bigcirc}$, $\mathbf{CA}_{\boxplus}$, and $CA_{\boxtimes}$, respectively. The details of ROI region drawn by the red square are shown in Fig. 5.

the reconstructed spectral images at 6 out 24 wavelength bands. The details of the ROIs drawn by the red squares are magnified and shown in Fig. 5. It is found that the use of the proposed misaligned CA in CASSI system can

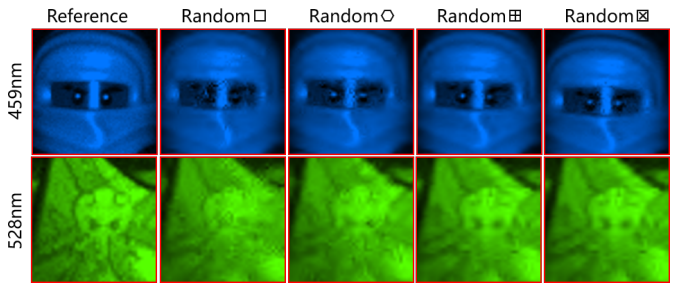

Fig. 5: Zoom-in counterparts of ROIs in Fig. 4. Left to right: the reference images, and the images reconstructed using random $CA_{\square}$, $CA_{\bigcirc}$, $\mathbf{CA}_{\boxplus}$, and $CA_{\boxtimes}$, respectively

reduce the reconstruction error and obtain reconstruction results closer to the reference images.

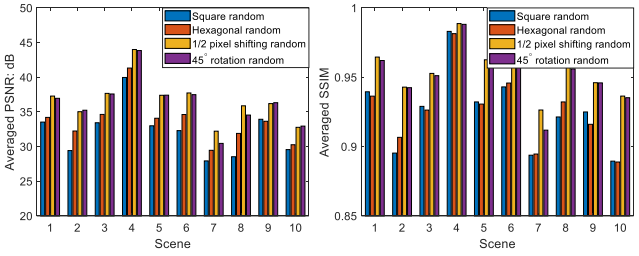

Fig. 6: Quantitative comparison of the reconstructed spectral images for different input scenes.

We also evaluate the proposed method on 10 input scenes from the ICVL dataset [12]. Figure 6 presents the averaged PSNR values and SSIM values of the reconstructed spectral images that use the above four types of coded apertures. It can be seen that the proposed $CA_{\boxplus}$ and $CA_{\boxtimes}$ overperform the competitive methods.

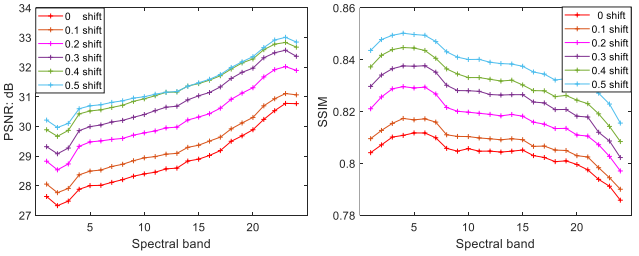

Fig. 7: Quantitative comparison of the reconstructed spectral images using different pixel shift lengths.

As for different pixel shifting lengths, we conducted the experiment and reported the results in Fig. 7, where the zero shift is equal to the regular $CA_{\square}$. It is found that as the shifting length increased from zero to half pixel length, the averaged PSNR and SSIM value of the reconstructed images get improved up to 2.55dB and 3.84%.

Spatiotemporal blue noise CAs have been shown to be the optimal CAs for multiple CASSI projections, which satisfy the criterion of restricted isometry property (RIP) with a high probability [6], [10]. Therefore, we also evaluate the proposed misalignment approach on the

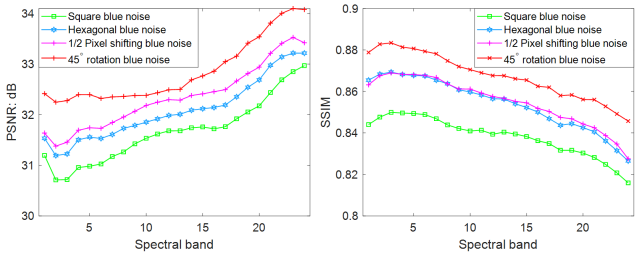

Fig. 8: Quantitative comparison of the reconstructed spectral images using blue noise CAs at 24 wavelength bands. Left and right are the PSNR values and the SSIM values of the reconstructed images, respectively.

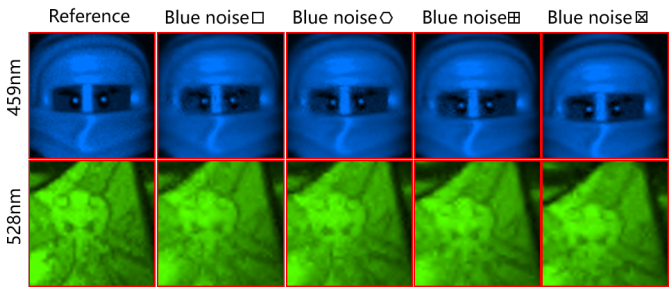

Fig. 10: Zoom-in counterparts of ROIs in Fig. 9. Left to right: the reference images, and the images reconstructed using blue noise $CA_{\square}$, $CA_{\bigcirc}$, $\mathbf{CA}_{\boxplus}$, and $CA_{\boxtimes}$, respectively.

blue noise CAs. The experiment setup remains the same except that the random CAs used in 10 snapshots are replaced with the spatiotemporal blue noise CAs, and the constant τ in (5) is empirically set to 4e-5, 2.5-5, 1.5e-5, and 0.8e-5 for the blue noise $CA_{\square}$, $CA_{\bigcirc}$, $CA_{\boxplus}$, and $CA_{\boxtimes}$, respectively. Figure 8 presents the PSNR values and SSIM

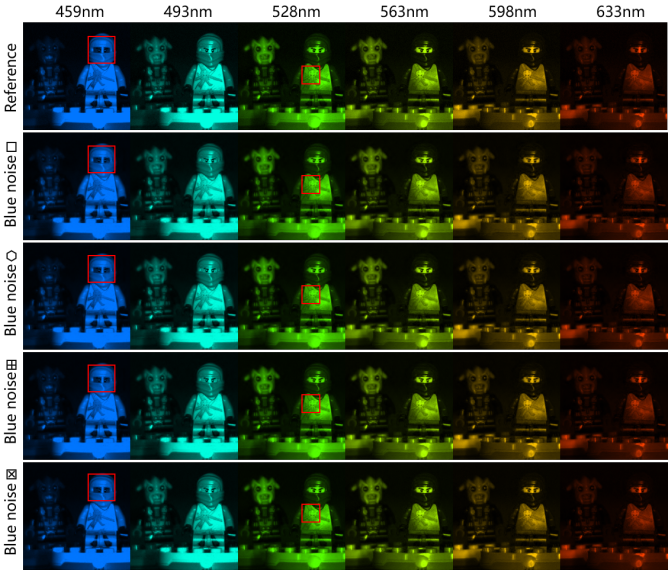

Fig. 9: Visual comparison of the reconstructed spectral images at 6 out 24 wavelength bands. Left to right: The selected wavelength bands. Top to bottom: The reference images, and the images reconstructed using blue noise $CA_{\square}$, $CA_{\bigcirc}$, $\mathbf{CA}_{\boxplus}$, and $CA_{\boxtimes}$, respectively. The details of ROI region drawn by the red square are shown in Fig. 10.

values of the reconstructed spectral images that use the blue noise $CA_{\square}$, $CA_{\bigcirc}$, $\mathbf{CA}_{\boxplus}$, and $CA_{\boxtimes}$, respectively. The corresponding average PSNR values at the 24 wavelength bands are 31.67dB, 32.08dB, 32.34dB, and 32.85dB. The corresponding average SSIM values are 0.8382, 0.8552, 0.8540, and 0.8674, respectively. The reconstructed spectral images at 6 out 24 wavelength bands as well as the ROIs drawn by red squares are presented in Fig. 9 and Fig. 10, respectively. It is found that the reconstruction performance can be further improved after applying the proposed misalignment approach to the CASSI system with the blue noise CAs.

IV. Conclusions

In summary, we propose a simple yet effective approach to improving the reconstruction performance of the CASSI system. It utilizes the misalignment between the CA and the FPA to introduce an equivalent grayscale modulation and subsequently enhances the sensing ability of the CASSI system. The effectiveness has been demonstrated by numerical experiments on both the random coded apertures and blue noise coded apertures.

References

[1] D. J. Brady, Optical imaging and spectroscopy. John Wiley & Sons, 2009.
[2] J. M. Bioucas-Dias, A. Plaza, G. Camps-Valls, P. Scheunders, N. Nasrabadi, and J. Chanussot, "Hyperspectral remote sensing data analysis and future challenges," IEEE Geoscience and remote sensing magazine, vol. 1, no. 2, pp. 6–36, 2013.
[3] N. Gat, "Imaging spectroscopy using tunable filters: a review," Wavelet Applications VII, vol. 4056, pp. 50–64, 2000.
[4] G. R. Arce, D. J. Brady, L. Carin, H. Arguello, and D. S. Kittle, "Compressive coded aperture spectral imaging: An introduction," IEEE Signal Processing Magazine, vol. 31, no. 1, pp. 105–115, 2013.
[5] A. Wagadarikar, R. John, R. Willett, and D. Brady, "Single disperser design for coded aperture snapshot spectral imaging," Applied Optics, vol. 47, no. 10, p. B44, 2008.
[6] C. V. Correa, H. Arguello, and G. R. Arce, "Spatiotemporal blue noise coded aperture design for multi-shot compressive spectral imaging," Journal of the Optical Society of America A, vol. 33, no. 12, p. 2312, 2016.
[7] H. Arguello, H. Rueda, Y. Wu, D. W. Prather, and G. R. Arce, "Higher-order computational model for coded aperture spectral imaging," Applied Optics, vol. 52, no. 10, 2013.
[8] C. Fu, M. L. Don, and G. R. Arce, "Compressive spectral imaging via polar coded aperture," IEEE Transactions on Computational Imaging, vol. 3, no. 3, pp. 408–420, 2016.
[9] O. F. Kar and F. S. Oktem, "Compressive spectral imaging with diffractive lenses," Optics Letters, vol. 44, no. 18, pp. 4582–4585, 2019.
[10] H. Zhang, X. Ma, D. L. Lau, J. Zhu, and G. R. Arce, "Compressive spectral imaging based on hexagonal blue noise coded apertures," IEEE Transactions on Computational Imaging, vol. 6, pp. 749–763, 2020.
[11] M. A. Figueiredo, R. D. Nowak, and S. J. Wright, "Gradient projection for sparse reconstruction: Application to compressed sensing and other inverse problems," IEEE Journal of selected topics in signal processing, vol. 1, no. 4, pp. 586–597, 2007.
[12] B. Arad and O. Ben-Shahar, "Sparse recovery of hyperspectral signal from natural rgb images," in European Conference on Computer Vision. Springer, 2016, pp. 19–34.